J Mater Sci (2009) 44:3694–3701
DOI 10.1007/s10853-009-3494-8

# Tensile behaviors of polyamide 6/UHLE blends

**Hongjun Luo · Zhuo Fu · Bo Jing · Jian Shi · Xiaoxuan Zou · Wenli Dai**

Received: 13 January 2009 / Accepted: 13 April 2009 / Published online: 5 May 2009


**Abstract** In this article, tensile behaviors of polyamide 6 and polyolefin blends were studied. Differential scanning calorimeter (DSC) was used to investigate the melting behaviors of injection-molded specimens and corresponding post-tensile tested specimens. As a result, the content of polyolefin blend, water, and anneal time has strong incidences on tensile behaviors of polyamide 6 blends. Double yielding was found in several blends under different conditions. DSC results showed that there are changes of crystal structure during tensile deformation. Finally, the origin of double yielding is detected to be related to polyamide 6.

## Introduction

Tensile deformation is a universal phenomenon. It will happen even at three-point bend testing. Typically, various deformation characteristics can be found in the different deformation stages [1]. Hiss [2] found four characteristic points where the differential compliance changes during the study of uniaxial drawing of polyethylene (PE) and related copolymer. On the basis of numerous observations, Na et al. [3] introduced three critical points on tensile stress–strain curves of semi-crystalline polymers.

A large number of studies have been carried out to present the mechanism of necking phenomenon of ductile polymers [4–8]. In general, necking will take place in a tensile specimen of a ductile material during large elastic–plastic deformation, and it will lead to localized deformation behavior in the necked region and finally to rupture at the neck section. On micro- and sub-microscales, the necking phenomenon is associated with micromechanisms of strain localization, such as crazing and shearing band, which causes a change in the morphology of the material where a spherulitic structure transforms into a fibrillar one [9], or a process of disintegration of lamellar crystal accompanied by lamellar fragmentation [10]. During stretching, this change occurs through shearing and fragmentation of the crystalline lamellae into blocks, which rearrange into the form of highly oriented parallel microfibrils.

As a particular phenomenon, double yielding will occur during tensile deformation under certain conditions such as the appropriate structure of material and strain rates. It is well known that double yielding is a general phenomenon to be expected in semicrystalline polymers but not in amorphous ones [11–13]. However, recently, double yielding was found in a styrene/butadiene star block copolymer by Adhikari et al. [14], in polycarbonate fibril/PE by Li et al. [15], and also in polyamide 6 (PA6)/K resin by Jing [16].

During the last two decades, many studies have been carried out to examine double yielding behaviors and their mechanisms of PA6 and PE [11, 12, 17, 18]. However, there are no references reporting whether double yielding exists in two semi-crystalline polymer blends. In this article, PA6 was modified by UHLE, which is a blend

H. Luo · Z. Fu · J. Shi · W. Dai
Chemistry College, Xiangtan University, Xiangtan 411105, Hunan, China

B. Jing · W. Dai (✉)
Key Laboratory of Polymeric Materials and Application Technology, Xiangtan University, Xiangtan 411105, Hunan, China
e-mail: Wli-d@163.com; wenlidai06@126.com

X. Zou
Key Laboratory of Advanced Functional Polymeric Materials, Xiangtan University, College of Hunan Province, Xiangtan 411105, China

composite of ultra-high molecular weight polyethylene (UHMWPE), high density polyethylene (HDPE), linear low density polyethylene (LLDPE), and ethylene–acrylic acid copolymer (EAA). EAA was used here as a compatilizer of PA6 and PE [19, 20]. In our primary study, double yielding was also found in PA6/UHLE blends, which induced us to investigate the origin of double yielding. Therefore, we will study the incidences of UHLE content, water, and anneal time on tensile behaviors of PA6/UHLE blends.

## Experiment

### Materials

The materials used in this study were PA6 (YH3400; Sinopec Baling Compony), HDPE (MH 602; SPC.), EAA (6100; the Dow Chemical Company), LLDPE (DFDA-7042; JPC.), and UHMWPE (FK550; Wuxi Fukun Chemical CO. LTD).

### Blends and specimens preparation

Before being mixed, PA6 and the other four materials were dried at 100 and 70 °C, respectively, for 4 h in a vacuum oven. UHMWPE, HDPE, LLDPE, and EAA were first blended with the weight ratio of 20/60/10/10 in twin-screw co-rotating extruder, and UHLE was short for the four polymers blend. Then UHLE was dried at 80 °C for 2 h in a vacuum oven. PA6 and UHLE were mixed in twin-screw co-rotating extruder (made by Nanjing Rubber & Plastic Machinery Plant) with the PA6/UHLE weight ratios of 98/2, 95/5, 90/10, 85/15, and 80/20. The temperatures of heating zones were set between 210 and 240 °C. The dumbbell tensile specimens (NC specimens) (120 mm × 6 mm × 4 mm) were injection molded after drying for 4 h at 100 °C on a Haitian injection-molding machine (HT B80) at a temperature range of 220–250 °C from the feed zone to the nozzle. In order to invest the influence of moisture and anneal on tensile behaviors of PA6/UHLE blends, NC specimens were treated in two ways: water treatment (WT) and thermal treatment (TT). WT specimens are those that obtained when NC specimens were soaked in water for 24 h at the temperatures of 27 (RT), 50, and 90 °C. Similarly, TT specimens are those when NC specimens were kept in an oven at the temperature of 110 °C for 15 and 30 h.

### Tensile tests

Tensile tests were carried out at 26 °C using Instron universal testing machine (RG D-5) equipped with a 5-kN load cell at a crosshead speed of 50 mm/min for all the specimens. The tensile tests are expressed in terms of nominal stress $\sigma = F/A_0$, where $A_0$ is the initial cross-sectional area, and the nominal strain $\varepsilon = (l - l_0)/l_0 \times 100\%$, where $l$ and $l_0$ refer to the overall gauge section. An infrared camera [6] was used to capture the temperature distribution during tensile deformation of NC neat PA6 specimen. The results are shown in Fig. 1, which indicates the temperature evolvement of PA6 specimen during

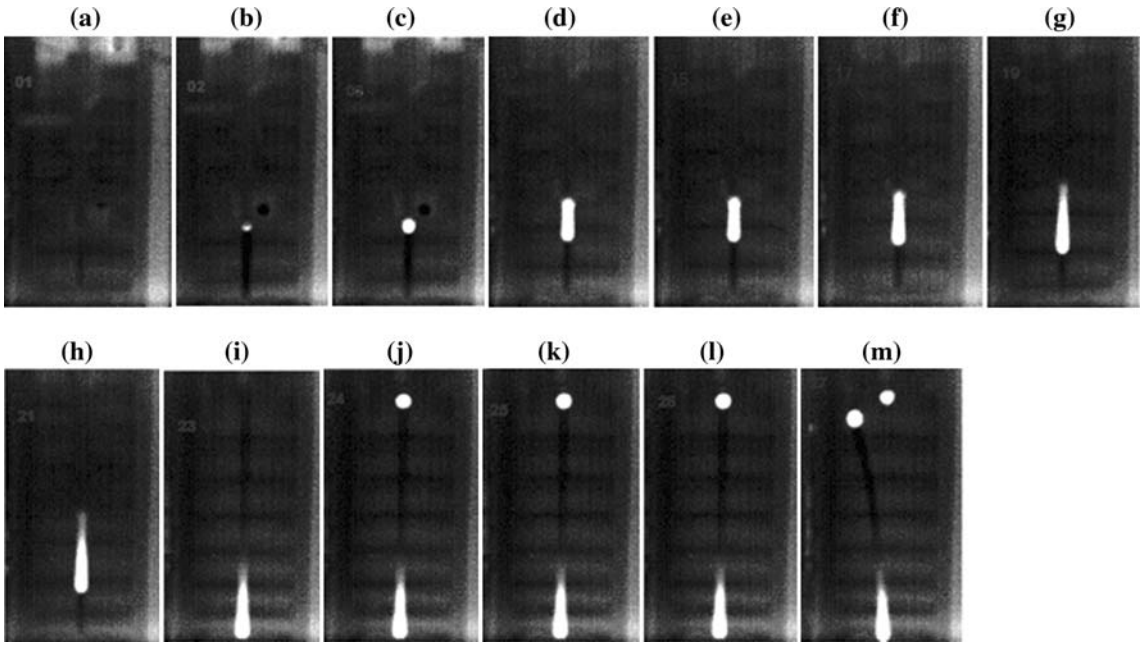


**Fig. 1** Temperature evolvement of NC neat PA6 specimen during tensile defamation

tensile deformation. The temperature of white region is higher than that of black region, being mainly caused by the friction of polymer molecules during necking.

### Differential scanning calorimeter (DSC)

Differential scanning calorimeter (DSC) was used to characterize the melting behavior of the original and post-deformation PA6/UHLE specimens. Samples taken both from injection-molded specimens (IM-specimens) and post-tensile tested specimens (PT-specimens) under NC were tested using a Modulated DSC from TA Instruments, model DSCQ10. The samples were only heated from room temperature up to 250 °C for PA6/UHLE and to 200 °C for UHLE for one time. Four PA6/UHLE blends were tested: 100/0, 95/5, 85/15, and 0/100.

## Results and discussion

### Tensile behavior of neat PA6

Figure 2 shows the typical engineering tensile stress–strain curve of NC neat PA6 specimen. Considering the stress–strain curve of neat PA6 only, we can clearly see that tensile deformation of neat PA6 underwent four stages. In the initial stage, elastic deformation took place until the yielding point with specimen dimension decreasing homogeneously, which is associated with Fig. 1a, where the whole region is black, that is to say, there is no heat produced from the slip of molecules from each other. Second, shear yielding deformation and following necking, marked with appearance of a white point in Fig. 1b and then the white regions extended from Fig. 1c–f, occurred when tensile stress is higher than yielding strength. During necking, there were two yielding points in tensile stress–strain curve. The first yielding point occurred at the strain of about 11.5% and the second at about 25%. Third, neat PA6 displayed a constant stress plateau region that is accompanied by neck propagation (this process is also named cold draw) when local neck achieved the minimum dimension. From Fig. 1g–i, the white region kept almost the same dimension and shape rather than from being further enlarged, because of heat transfer from specimen to environment. Finally, tensile strain hardening occurred after complete necking and specimen fracture. There is a separate white point existing in the fracture region shown in Fig. 1j–k, l while there are two white points in the completely fractured region shown in Fig. 1m.

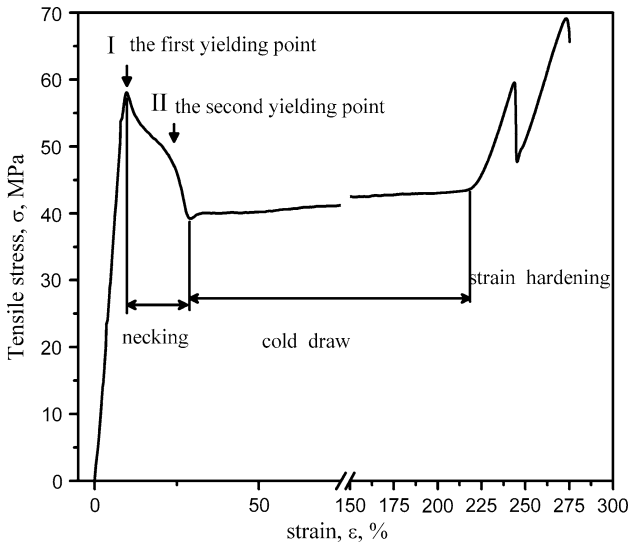


**Fig. 2** Typical engineering tensile stress–strain curves of NC neat P6 specimen

### The influence of UHLE content on tensile behavior of PA/UHLE blends

Figure 3 shows the engineering tensile stress–strain curves of NC P6/UHLE specimens. As shown in Fig. 3, the tensile behaviors of PA6/UHLE blends are similar to that of neat PA6 specimen. There are no steady necking processes in UHLE and 80/20 PA6/UHLE blends. The strain at the yielding point of UHLE is about 25% while that at the first yielding point of PA6/UHLE blends is about 11.5%. This demonstrated that the yielding in PA6/UHLE blends must be initiated by PA6. There are double yielding behaviors in 98/2, 95/5, and 90/10 PA6/UHLE blends, and UHLE seems to depress the double yielding behavior so that there is no double yielding point in stress–strain curves of 85/15 and 80/20.

Prasath Balamurugan [8] used to determine that the instability in the yielding process can be defined by the index of cold drawing (ICD), which is the ratio of the upper yield stress and the lower yield stress (draw stress). The larger the ICD, the shaper or the more localized the

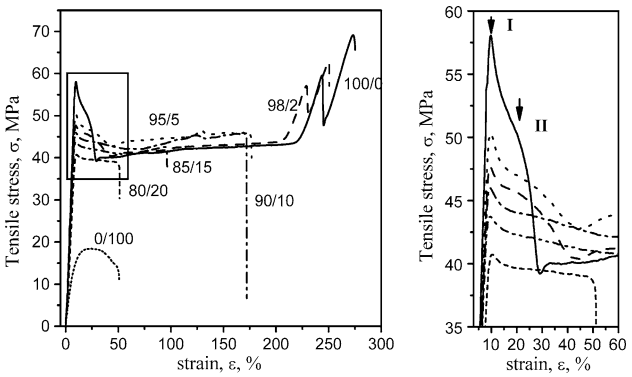


**Fig. 3** Engineering tensile stress–strain curves of NC PA6/UHLE blends

**Table 1** Tensile properties of NC PA6/UHLE blends

| PA6/UHLE | 100/0 | 98/2 | 95/5 | 90/10 | 85/15 | 80/20 | 0/100 |
|---|---|---|---|---|---|---|---|
| $E$ (MPa) | 664.2 | 608.9 | 621.6 | 572.8 | 554.6 | 493.5 | 199.4 |
| $\sigma_y$ (MPa) | 56.5 | 47.7 | 51.5 | 46.2 | 43.7 | 40.7 | 17.1 |
| ICD | 1.40 | 1.15 | 1.14 | 1.09 | 1.07 | – | – |

$E$ is the elastic modulus; $\sigma_y$ the tensile yielding stress; ICD the index of cold draw

necking. Increment of entangled molecules in amorphous region will restrain shrinkage of cross-sectional area of specimens. It also accords with our result in terms of the ICD. With the UHLE content increment, the ICD got closer to 1, as shown in Table 1. In other words, necking is less local and the neck dimension increases. Table 1 exhibits the tensile properties of NC PA6/UHLE blends. Certainly, there is a strong influence of UHLE on elastic modulus ($E$), tensile yielding stress($\sigma_y$), and the ICD.

In order to compare melting behaviors of deformed and original PA6/UHLE specimens, DSC heating curves of PA6/UHLE blends used injection-molded specimens (IM specimens) and post-tensile tested specimens (PT specimens) were obtained and shown in Fig. 4. The black lines and dash lines mark IM and PT-specimens, respectively. Considering that there was no neck in UHLE specimen, the DSC heating curve of UHLE has not been taken. From Fig. 4, we can see that there are two melt peaks on the heating curves of PA6/UHLE blends. The first peak occurred at about 135 °C, which corresponds to the melting peak of UHLE and the second peak at about 225 °C, which corresponds to the melting peak of PA6. In fact, UHLE content must have a little influence on crystallinity of PA6 as there is a shift of melt peak to higher temperature in small scale. In contrast, the second melt peaks of PT-specimens in heating curves are at temperatures about 8 °C higher than those of IM-specimens. This shows that there

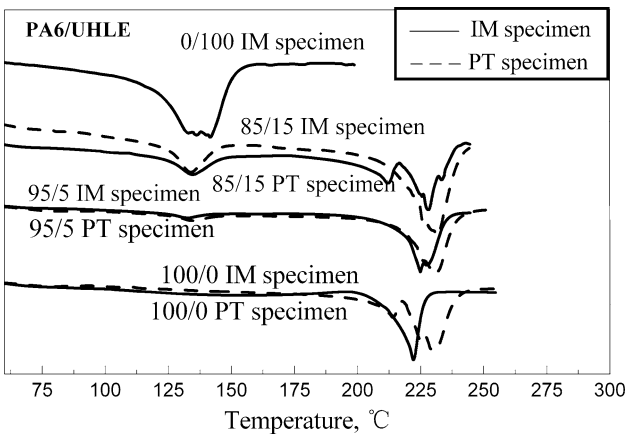


**Fig. 4** DSC heating scans of injection-molded and post-tensile tested PA6/UHLE specimens

were changes in crystal structure from γ-crystal to α-crystal [21]. However, no changes were exhibited in melt peaks of UHLE.

## The influence of water on tensile behaviors of PA6/UHLE

Table 2 exhibits the water absorption ratio (WAR) of PA6/UHLE blends at three water temperatures. PA6 has high ability of water absorption, but UHLE is hydrophobic. Therefore, when UHLE was added into PA6, more content of UHLE, lower water absorption ratios are observed of PA6/UHLE blends. Elevating temperature of water (the $T$g of PA6 is about 45 °C), PA6 chain segment movement intensified, and more water can permeate into the inner of specimens. As a result, more water was absorbed by specimens. At the same time, the ability of UHLE chain segment movement was intensified and the hydrophobicity of UHLE became greater, which resulted in water absorption of UHLE decreasing with increasing the water temperature. By this means, we got tensile specimens with different water absorption ratios after treatment at different water temperatures.

Figure 5 displays the engineering tensile stress–strain curves of WT P6/UHLE specimens at three water temperatures: (a) (RT = 27 °C), (b) (50 °C), and (c) (90 °C), respectively. Figure 5a, b and c on comparison show strong incidences of water on tensile behavior of PA6 and its blends, but little influence on UHLE specimens. In general, elastic modulus and tensile stress sharply decrease and tensile ratio at break increases as the water temperature increases for all the specimens except for UHLE, as shown in Table 3. At the same time, the draw ratio got decreased, that is to say, the tensile behaviors underwent more and more deformations to form rubber-like polymers. For the neck specimen, the dimension of neck zone increased with higher water absorption and necking was completed at lower strain followed by strain hardening. Also, the draw stress of PA6/UHLE blends is always higher than that of neat PA6. However, necking always exists in PA6 specimen no matter what the temperature is. Most importantly, there are serious changes in yielding. Two yield points can also be observed before necking in both neat PA6 and 95/5

**Table 2** Water absorption of PA6/UHLE blends at three water temperatures

| PA6/UHLE | 0/100 | 100/0 | 95/5 | 90/10 | 85/15 | 80/20 |
|---|---|---|---|---|---|---|
| WAR[a] at RT (%) | 0.33 | 1.78 | 1.66 | 1.45 | 1.33 | 1.15 |
| WAR at 50 °C (%) | 0.26 | 3.10 | 3.14 | 2.82 | 1.39 | 2.25 |
| WAR at 90 °C (%) | 0.07 | 4.74 | 5.15 | 4.68 | 4.15 | 3.71 |

[a] WAR is water absorption ratio

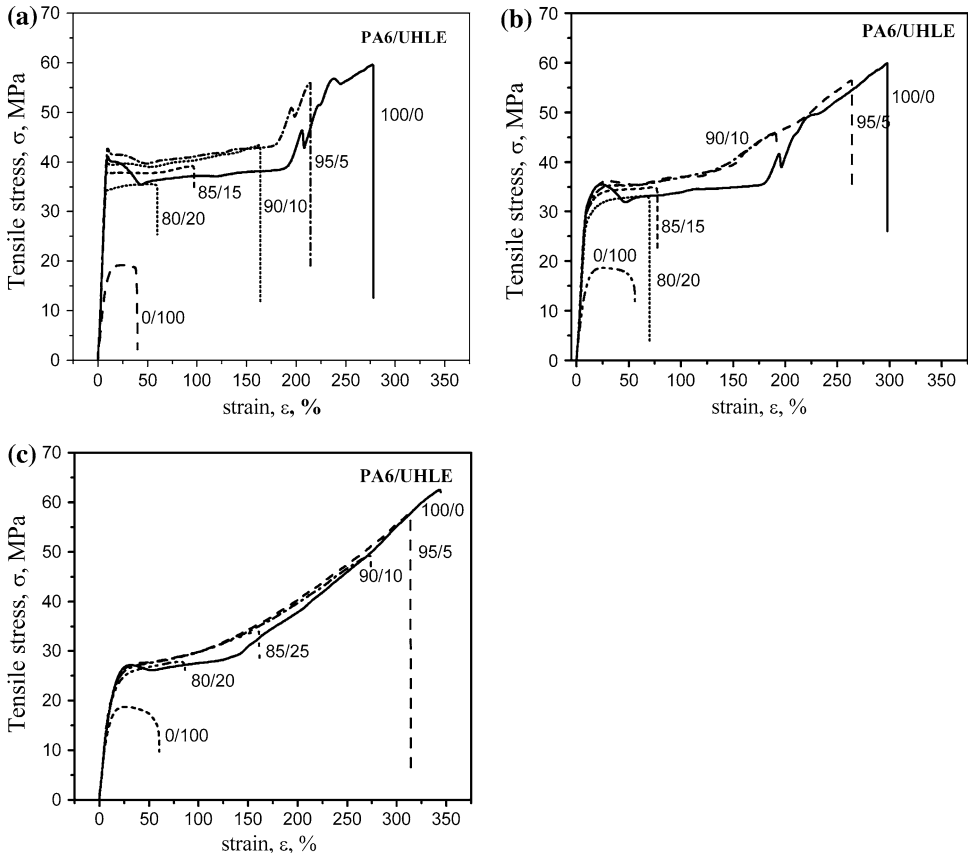


**Fig. 5** Engineering tensile stress–strain curves of WT PA6/UHLE blends; the temperatures of water treatment are **a** (RT), **b** (50 °C) and **c** (90 °C), respectively

**Table 3** The tensile properties of WT PA6/UHLE blends

| | *A*/*B*/*C* | | | | | |
|---|---|---|---|---|---|---|
| PA6/UHLE: | 100/0 | 95/5 | 90/10 | 85/15 | 80/20 | 0/100 |
| *E* (MPa) | 509/422/121 | 553/410/125 | 512/412/155 | 515/400/240 | 456/355/232 | 206/199/190 |
| $\sigma_y$ (MPa) | 41/35/27 | 43/36/27 | 40/35/26 | 38/34/26 | 34/31/25 | 19/18 |

*E* is the elastic modulus; $\sigma_y$ the tensile yielding stress; *A*, *B* and *C*, respectively, represent water temperature of 27, 50, and 90 °C

blend in Fig. 5a and then the first yield points disappear, i.e., there is only one yield point at strain of about 25% in each stress–strain curves, for the strain usually corresponds to that where the second yield point occurred as shown in Fig. 2. According to this, water more likely depresses the first yielding of PA6 and its blends. On the other hand, it can further be confirmed that double yielding is mainly initiated by PA6.

## The influence of anneal treatment on tensile behaviors of PA6/UHLE

Figure 6a, b presents engineering tensile stress–strain curves of TT PA6/UHLE specimens treated for 15 h and 30 h, respectively. From Fig. 6a, it can be seen that in the initiation stage, all the blends suffered elastic deformation, which were followed by yielding deformation, i.e., necking. It is evident that there were two yield points before necking process in the early stage. The first yield point occurred at strain of 11.5%, where no distinct neck occurred, and the second one occurred at the strains of about 27%. After the second yield point, stress decreased almost vertically for neat PA6 specimens. Then PA6 specimen went on necking with a constant stress. Finally, PA6 specimen fractured before strain hardening, which might be caused by the defect generated during anneal. As regards the other PA6/UHLE blends, there are still double yield points in these blends excluding 80/20 blend. Figure 6b reveals that the specimens experienced the similar deformations as shown in Fig. 6a. The differences are that stresses at the second yielding point are lower than that at the first yielding point, and the stress downtrend after the

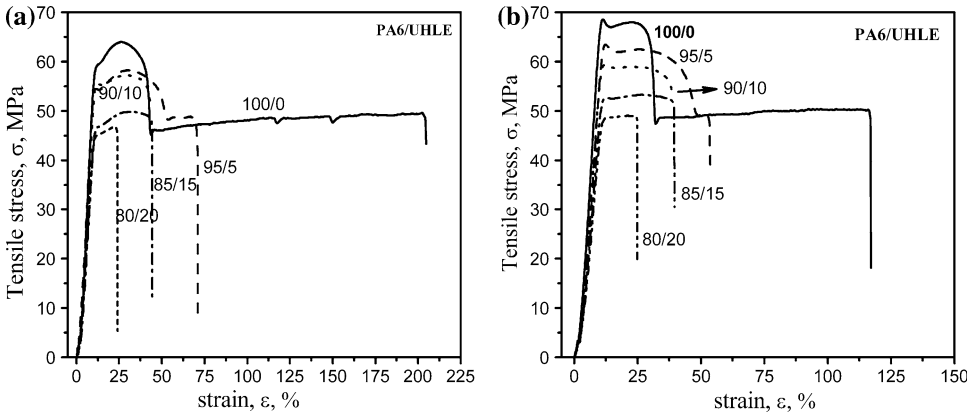


**Fig. 6** Engineering tensile stress–strain curves of TT PA6/UHLE blends, **a** and **b**, treated for 15 h and 30 h, respectively

second yielding point is even sharper than that shown in Fig. 6b. In addition, there occurred a clear necking in small scale between the two yielding points as shown in Fig. 6b.

## Discussion

### Explanation of influence on tensile properties

Hong et al. [4] recently proposed a model treating for tensile deformation of semicrystalline polymers, in which the drawing stress is considered as being composed of these three components, namely (i) the forces transmitted by the skeleton of crystal blocks, (ii) the force brought up by the stretched amorphous network, and (iii) the force arising from the viscosity. In short, elasticity in semicrystalline polymers arises from the contributions of both the network of entangled chains in the amorphous parts of the sample and the skeleton of coupled crystalline blocks. This model can be used to explain the influence of UHLE, water, and anneal on tensile properties, such as elastic modulus and yielding stress. When the content of soft UHLE blend is increased, the concentration of PA6 will decrease and the amorphous regions widen. As a result, the tensile modulus decreases step-by-step as shown in Table 1. Because of more small water molecule getting into the specimens treated by water, which affects the internal structure of specimens and can activate macromolecular segment, tensile modulus of WTC PA6/UHLE blends reduced much. The glass transition temperature of PA6 is about 45 °C, so that when the specimens are thermally treated at 110 °C, both motion ability of PA6 molecule segments and the crystalline degree will increase. Along with the increment of treated time, crystallization was nearer to perfection, and as a result, the tensile modulus, tensile stress, and tensile yielding increase, but tension ratios decrease, resulting from less amorphous regions in TTC specimens.

The moment yielding deformation begins, crystal damages and laminar crystallites slip to each other, and to the molecules in amorphous regions orient, at the same time, causing friction of molecules generate heat, which can be proved from the other graphs in Fig. 1. Although the oriented molecules and laminar crystallites or re-crystallites (see Fig. 3) increase the resistance of stress deformation, cross-sectional area of local necking region reduces much, which causes the stress decrease. It is interesting to note that gradient of tensile stress is correlated with the slip rate of laminar crystallites during local necking. The latter determines the shape of local necking region. In other words, gradient of tensile stress corresponds to the time needed by the original area to change into the minimum area, i.e., neck area. Increment of entangled molecules in amorphous region will restrain shrinkage of cross-sectional area of specimens. As a result of entangled molecules of UHLE, the gradient of tensile stress cuts down as the content of UHLE blend increases. This phenomenon can be clearly seen in all the specimens. Certainly, there is no constant stress plateau region always for all the specimens, which may be due to several reasons: polyolefin molecules cannot endure high-level stress and fracture; either voids exist in specimen during injection-molding or are initiated by tensile deformation; UHLE cannot be dispersed evenly.

### Double yielding

In order to discuss the special double yielding phenomenon clearly, the tensile stress–strain curves of neat PA6 specimens under various conditions were drawn out from the above figures to create a new graph, see Fig. 7. In Fig. 7, the stress–strain curves drawn here do not include the segment over 70% in strain for the sake of more clearly demonstrated curves before necking. From this figure, we can clearly observe that there are double yielding points in all specimens excluding specimen under WT at 50 and 90 °C. The double yielding phenomenon is also found in the other PA6/UHLE blends. In general, the first yielding point of NC, TT specimens occurred at the strain about 11.5% and the second one at about 25%. Seguela and

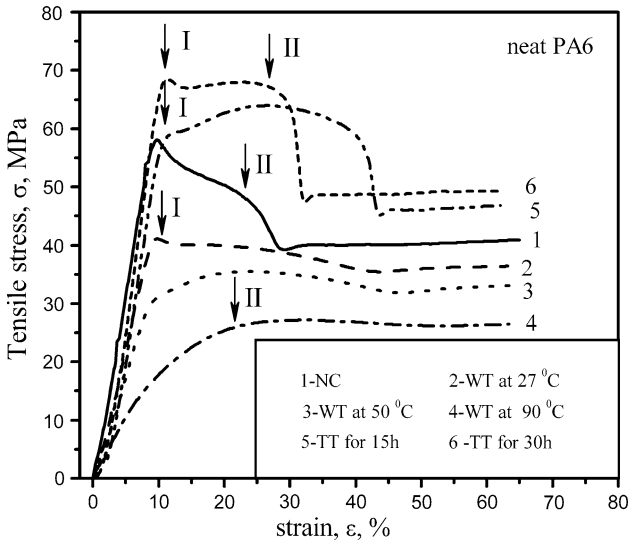


**Fig. 7** Tensile behaviors of neat PA6 specimens under various conditions

Rietsch [22] have proposed that the slip of the crystal blocks and the homogeneous shear of these blocks could explain the appearance of the two yield maxima observed. For semicrystalline polymers, the first yield point was attributed to the slip of the crystal blocks past each other in the mosaic crystalline structure (called the heterogeneous slip); the second yield point was attributed to the homogeneous shear of the crystal block (called as homogeneous slip), which marks the onset of effectively irrecoverable plastic deformation. This case is truly reflected in our results. UHLE might have depressed the second yielding for more entangled PE molecules dispersing in PA6/UHLE specimens, which can disturb the homogeneous shear of the crystal blocks, while water should have affected the structure of PA6/UHLE specimens and depressed the first yielding. Shan [18] have studied the effect of crystallinity level on the double yielding behavior of PA6. They found that the second yielding stresses are higher than the first yielding stresses when the specimens were annealed at 100 °C for a duration from 1 to 13 h, which is similar to the present result of TT specimen for 15 h. However, the second yielding stress of the TT specimens for 30 h is again lower than the first one. They consider that the second yield point is much more apparent with a decrease of the crystalline degree of the specimens. However, after reviewing "The engineering stress–strain curves of PA6 with different annealing times ($T = 100$ °C)" in their work, it is clear that the elastic modulus and yielding stress at both yield points of annealed PA6 are higher than those of unannealed PA6. In this sense, compared with Hong's model, it should raise doubt over "decrease of the crystalline degree as anneal time increase".

In general, although it is widely accepted that double yielding is thermal strain rate controlled, the origin of double yielding may be related to the structure of PA6 in this article, which can be affected by UHLE content, water, and anneal.

### Question put forward from the results

Interestingly, there are indeed re-necking during strain hardening of NC, WT at 27 and 50 °C neat PA6 specimens, NC PA6/UHLE (98/2) and WT at 27 °C PA6/UHLE (95/5) specimens. The onset of re-necking is associated with the turning point in their latest parts of stress–strain curves. However, to the best of our knowledge, no one has reported this phenomenon and explained why it happens. In our opinion, the reason may be that the structure is heterogeneous along the injection-molded specimens.

## Conclusion

In this article, tensile behaviors of PA6/UHLE blends were studied using NC, WT, and TT specimens. UHLE, water, and anneal strongly affected the tensile behaviors of PA6/UHLE blends. Elastic modulus and tensile yielding stress decrease as the UHLE content and WAR increase. In contrast, they changed in the opposite manner when anneal time increases. Tensile ratios at break decreased with UHLE content and anneal time, and increased with WAR. Particularly, double yielding can be observed in several specimens and the first yield point occurred at the strain of about 11.5% and the second one at about 25%. UHLE and water can depress the second yielding and the first yielding, respectively. However, the anneal time would intensify both yield point. In conclusion, the origin of double yielding is related to the structure of PA6 matrix.

**Acknowledgement** This project was supported by Hunan Provincial Natural Science Foundation of China, 07J J6016

## References

1. Haward RN (1993) Macromolecules 26:5860
2. Hiss R, Hobeika S, Lynn C, Strobl G (1999) Macromolecules 32:4390
3. Na B, Zhang Q, Fu Q (2006) Macromolecules 39:2584
4. Hong K, Rastogi A, Strobl G (2004) Macromolecules 37:10165
5. Brünig M (1998) Finite Elem Anal Des 28:303
6. Wattrisse B, Muracciole JM, Chrysochoos A (2002) Int J Therm Sci 41:422
7. Chudnovsky A, Preston S (2002) Mech Res Commun 29:465
8. Prasath Balamurugan G, Maiti SN (2008) Polym Test 27:752
9. Peterlin A (1971) J Mater Sci 6:490. doi:10.1007/BF00550305
10. Nitta K, Takayanagi M (2000) J Polym Sci B Polym Phys 38:1037

11. Feijoo JL, Sanchez JJ, Mueller AJ (1997) J Mater Sci Lett 16:1721
12. Balsamo V, Müller AJ (1993) J Mater Sci Lett 12:1457
13. Brooks NW, Duckett RA, Ward IM (1995) J Rheol 39:425
14. Adhikari R (2004) Macromol Rapid Commun 25:653
15. Li ZM, Huang CG, Yang W, Yang MB, Huang R (2004) Macromol Mater Eng 289:1004
16. Jing B, Dai WL, Cao Q, Liu PS (2006) Polym Bull 57:359
17. Shan GF (2007) Polymer 48:2958
18. Shan GF (2006) Polym Test 25:452
19. Scaffaro R (2003) Polymer 44:6951
20. Jiang CH, Filippi S, Magagnini P (2003) Polymer 44:2411
21. Galeski A, Argon AS, Cohen RE (1988) Macromolecules 21:2761
22. Seguela R, Rietsch F (1990) J Mater Sci Lett 9:46